Research on the Nonlinear Response of the Rotor System with Bolted Joint with Spigot

Yongbo Ma[1(✉)], Jie Hong[1,2], Shaobao Feng[3], and Yanhong Ma[2]

[1] School of Energy and Power Engineering, Beihang University, Beijing 100191, People's Republic of China
mayongbo2020@163.com
[2] Research Institute of Aero-Engine, Beihang University, Beijing 100191, People's Republic of China
[3] AECC Shenyang Engine Design and Research Institute, Aero Engine (Group) Corporation of China, Shenyang 110015, People's Republic of China

Abstract. The bolted joint with spigot is the most common form of joint in the aero-engine rotor system. There will be slip damage at the spigot interface under the complex load, which will influence the dynamic characteristic of the rotor system. However, there are few researches on the spigot interface, so the mechanical characteristic of the non-continuous rotor system cannot be described accurately enough. In this paper, a new mechanical model of bolted joint with spigot has been proposed, which can accurately describe the force-displacement characteristic of the bolted joint with spigot. In addition, the dynamic characteristic of the non-continuous rotor system with the bolted joint with spigot has been calculated, which has been used to analyze the influence of the nonlinear characteristic on the rotor whirl. The results show that the slip process of the spigot interface can been divided into three stages: sticking, microslip and macroslip, with obvious nonlinear characteristic of stiffness, and there may be bifurcation phenomenon in the dynamic response of the non-continuous rotor system. In addition, the influence of the slip damage will vary according to the structure parameters and the excitation, which is necessary to be considered in the robust design of aero-engine rotor system.

Keywords: rotor dynamics · Nonlinear response · spigot interface · Bolted joint

1 Introduction

The aero-engine rotor system usually consists of multiple components, and assembled by various joints [1, 2]. As shown in the Fig. 1, the bolted joint with spigot is one of the most common joints, which is beneficial to the high-speed rotors because of the higher centering accuracy and lower unbalance. However, affected by complex load, there may be slip damage at the interface of joints during operating, which will affect the rotor mechanical characteristic and seriously threaten to safety and stability of rotor system. Therefore, it's necessary to study the slip damage at the interface during operating, and analyze the impact on the dynamic characteristic of the rotor system.

F. Chu and Z. Qin (Eds.): IFToMM 2023, MMS 139, pp. 159–172, 2024.
https://doi.org/10.1007/978-3-031-40455-9_13

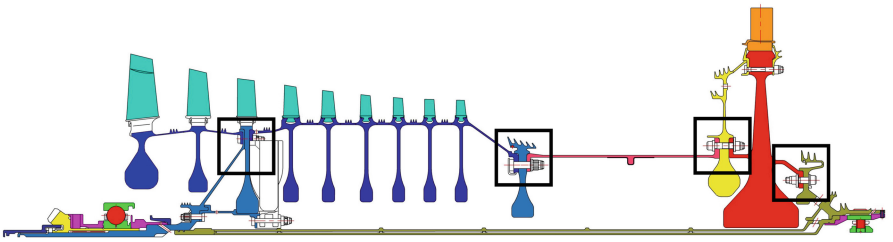

Fig. 1. The bolted joints with spigot in aero-engine rotor system

Different from the continuous structure system, the contact state at the interface of the joints will change under complex load, and affect the mechanical properties [3]. The development of contact mechanics, tribology and other disciplines, provided a solution for the interface contact. Matthew [4], from Sandia National Laboratory, divided the whole slip process into four stages: sticking, microslip, macroslip and pinning, by studying the bolted joints under the tangential force. Gaul [5] applied a periodic tangential load to the bolted joint, and found the contact state of the interface gradually changed from microslip to macroslip with the load increasing. Marshall [6] used a nonintrusive ultrasonic technique to quantify the contact pressure distribution in a bolted joint. The famous Iwan model [7, 8], which explained the nonlinear mechanical behavior of the contact interface, had become the most widely used phenomenological model.

Based on the research of contact state, extensive researches have been done on the joint mechanical characteristic. Argatov [9] derived the analytical nonlinear constitutive equation of bolted joint. Kim [10] established a fine finite element model of bolted joint by three-dimensional solid elements according to the actual size, obtained the interface stress distribution and structural deformation, and then studied the stiffness of the joint structures. Beaudoin [11] presented a new lump model that accounts for the nonlinear phenomena of partial clearance and friction, and had analytical parameters related to the flange geometry. Fan [12] established the model of bolted joint in aero-engine, revealed the mechanism of stiffness nonlinearity, and calculated the steady-state response of dual-rotor system when the stiffness of the joint structure is interval distributed. Yue [13] established the stiffness damage model of the rabbet joint structure and proposed the robust design method of the rabbet joint structure. Wang [14] established a detailed dynamic model of non-continuous rotor, and introduced interval analysis method.

Based on the research on the joint mechanical characteristic, the research on the rotor system with joints has also been carried out. Caddemi [15, 16] derived the closed-form solution method for the rotor system with singularity change in mechanical characteristic by generalized functions, and analyzed the dynamic characteristic of discontinuous rotor, and gives the analytical solution. Yang [17] analyzed the asymmetric and specific residual pre-tightening force of the bolts after the bolted joint operated, established the parametric excitation system of the time-varying stiffness of the aero-engine rotor system, and found the combined frequency in the rotor response. Chen [1] proposed a discontinuous rotor dynamics optimization method according to the joint stiffness characteristic. Dai [18] studied the rotor dynamic characteristic with the loose supports, and

proposed a dynamic optimization method for the multi-support flexible rotor system. Lei [19] established quantitative evaluation parameters based on interface deformation coordination, and optimized geometric characteristic parameters of rotor. However, there have been few studies about the spigot. Hong [20] established a slip damage mechanical model to analyze the stiffness loss in the aero-engine rotor system. Yu [21] established a nonlinear analysis model to describe the mechanical behavior of the aero-engine rotor under bending moment considering the spigot interface, and calculated the nonlinear stiffness and damping of the joint structure.

It can be found that there are sufficient studies on the joint mechanical characteristic, but the research on the bolted joint with spigot is relatively lacking. Aiming at the bolted joint with spigot in the aero-engine rotor system, the mechanical model has been proposed to analyze the slip damage during operating and the dynamic response of the non-continuous rotor system considering slip damage has been calculated in this paper.

2 Mechanical Model of Slip Damage at the Spigot Interface

In this section, the slippage of the joint interface under axial external load is modeled based on the classic Iwan model to describe the Force-Displacement characteristic of the bolted joint with the spigot.

2.1 The Distribution Function of Slippage at the Spigot Interface

There is usually a certain amount of interference at the spigot interface, to achieve the centering of the different components. The contact stress distribution at the spigot interface is generally complex, as shown in the Fig. 2, and the normal stress distribution has been roughly simplified as a quadratic distribution along the axial direction in this paper.

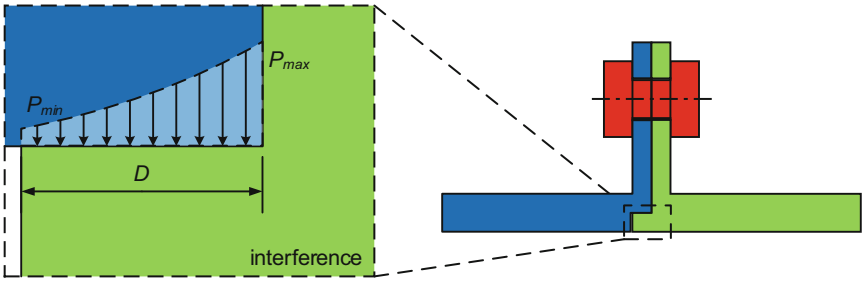

Fig. 2. The normal contact stress distribution at the spigot interface

Therefore, it is assumed that the normal contact stress distribution at the spigot interface is

$$P(d) = P_{\min} + (P_{\max} - P_{\min})\frac{d^2}{D^2} \tag{1}$$

where, D is the axial length of spigot interface, $P_{\max}$ and $P_{\min}$ are respectively the maximum and minimum of the normal contact stress at the spigot interface and d represents the axial position at the interface.

Thus, the maximum friction force for different positions can be provided is

$$\tau(d) = \mu\left[P_{\min} + (P_{\max} - P_{\min})\frac{d^2}{D^2}\right] \tag{2}$$

where, μ is the coefficient of friction of the spigot interface, which is regarded as a constant in this model.

The spigot interface will slip under the axial tension load. The relationship between slip area and critical slip position is

$$s(d) = d \cdot t \tag{3}$$

where, t is the width of spigot interface, d is the critical position at which slips.

By substituting Eq. (3) into Eq. (2), the maximum friction expressed in slip area can be obtained:

$$\tau(s) = \mu\left[P_{\min} + (P_{\max} - P_{\min})\left(\frac{s}{Dt}\right)^2\right] \tag{4}$$

Conversely, the slip area is expressed by the maximum friction:

$$s(\tau) = \begin{cases} 0 & 0 \le \tau < \mu P_{\min} \\ Dt\sqrt{\frac{\tau - \mu P_{\min}}{\mu(P_{\max} - P_{\min})}} & \mu P_{\min} \le \tau < \mu P_{\max} \\ Dt & \tau > \mu P_{\max} \end{cases} \tag{5}$$

Normalize the slip area:

$$\tilde{s}(\tau) = \frac{s(\tau)}{s_{\max}} = \begin{cases} 0 & 0 \le \tau < \mu P_{\min} \\ \sqrt{\frac{\tau - \mu P_{\min}}{\mu(P_{\max} - P_{\min})}} & \mu P_{\min} \le \tau < \mu P_{\max} \\ 1 & \tau > \mu P_{\max} \end{cases} \tag{6}$$

where, $s_{\max} = Dt$.

Taking the derivative of Eq. (6) with respect to τ:

$$\Psi(\tau) = \frac{d\tilde{s}(\tau)}{d\tau} = \frac{1}{2}[(\tau - \mu P_{\min})(\mu P_{\max} - \mu P_{\min})]^{-\frac{1}{2}} \quad \mu P_{\min} \le \tau \le \mu P_{\max} \tag{7}$$

2.2 Force-Displacement Relationship of Spigot Interface

W. D. Iwan [7, 8] had proposed a phenomenological model for the nonlinear mechanical behavior at the interface in 1966. Because of the simple structure and clear physical

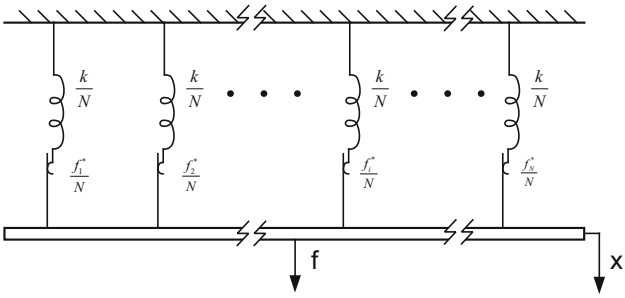

Fig. 3. Schematic diagram of the Iwan model

meaning, this model has been widely used and sufficiently developed in recent years. In this part, the Iwan model has been used to derive the force-displacement relationship of the contact interface.

The Iwan model includes multiple Jenkins elements, as shown in the Fig. 3, the friction force F and the displacement x satisfies

$$F(x) = \int_0^{kx} f^* \cdot \Psi(f^*) df^* + \int_{kx}^{\infty} kx \cdot \Psi(f^*) df^* \tag{8}$$

where, $\Psi(f^*)$ is the distribution function of the maximum friction provided by different Jenkins elements. In this model, it is considered that the relevant material parameters of the interface are the uniform, so it is assumed that the stiffness of each Jenkins element in the sticking stage is the same, $k_i = k$, $i = 1, 2, 3...$

Let $\tau = \lambda f^*$, substitute it into Eq. (7):

$$\Psi(f^*) = \frac{1}{2}\left[(\lambda f^* - \mu P_{\min})(\mu P_{\max} - \mu P_{\min})\right]^{-\frac{1}{2}} \quad \mu P_{\min} \le \tau \le \mu P_{\max} \tag{9}$$

Substitute Eq. (9) into Eq. (8), the force-displacement relationship of this model can be obtained.

where, $\lambda k \varphi_2 = \tau_{\max} = \mu P_{\max}$. φ_1 and φ_2 respectively indicate the critical displacement of mircroslip and macroslip at the spigot interface, and can be obtained:

$$\Psi(\varphi) = \frac{1}{2\lambda k\sqrt{\varphi_2 - \varphi_1}}(\varphi - \varphi_1)^{-\frac{1}{2}} \quad \varphi_1 \le \varphi \le \varphi_2 \tag{10}$$

Segalman [22, 23] proposed a coefficient to replace k in Eq. (8):

$$\rho(\varphi) = k^2 \cdot \Psi(\varphi) \quad \varphi = f/k \tag{11}$$

Substitute Eq. (11) into Eq. (9), the new expressions of Iwan model and interface contact normal stress distribution can be obtained respectively:

$$\rho(\varphi) = k^2 \bullet \Psi(\varphi) = \frac{k}{2\lambda\sqrt{(\varphi - \varphi_1)(\varphi_2 - \varphi_1)}} \quad \varphi_1 \le \varphi \le \varphi_2 \tag{12}$$

$$F(x) = \int_0^x \phi \bullet \rho(\phi) d\phi + \int_x^\infty x \bullet \rho(\phi) d\phi \tag{13}$$

and then:

$$\begin{cases} \int_0^{\varphi_1} \rho(\varphi) d\varphi = K_0 \\ \int_{\varphi_1}^{\varphi_2} \rho(\varphi) d\varphi = K_0 - K_\infty \\ \int_{\varphi_2}^{\infty} \rho(\varphi) d\varphi = K_\infty \end{cases} \tag{14}$$

where, K_0 represents the initial stiffness, K_∞ represents the residual stiffness.

Solve Eq. (14) and obtain the density function $\rho(\varphi)$:

$$\begin{aligned} \rho(\varphi) = K_0 \bullet \varphi \left[H(\varphi) - H(\varphi - \varphi_1) \right] \\ + \frac{K_0 - K_\infty}{2\sqrt{(\varphi - \varphi_1)(\varphi_2 - \varphi_1)}} \left[H(\varphi - \varphi_1) - H(\varphi - \varphi_2) \right] + K_\infty \delta(\varphi - \varphi_\infty) \end{aligned} \tag{15}$$

where, $H(\,)$ and $\delta(\,)$ are respectively the Heaviside function and the Dirac delta function.

Substitute Eq. (15) into Eq. (13) and obtain the force-displacement relationship is:

$$F(x) = \begin{cases} K_0 x & 0 \le x < \varphi_1 \\ K_0 x - \frac{2(K_0 - K_\infty)}{3\sqrt{\varphi_2 - \varphi_1}} (x - \varphi_1)^{\frac{3}{2}} & \varphi_1 \le x < \varphi_2 \\ \frac{1}{3}(K_0 - K_\infty)(2\varphi_1 + \varphi_2) + K_\infty x & \varphi_2 \le x \end{cases} \tag{16}$$

and the stiffness-displacement relationship is:

$$K(x) = \frac{dF(x)}{x} = \begin{cases} K_0 & 0 \le x < \varphi_1 \\ K_0 - \frac{(K_0 - K_\infty)}{\sqrt{\varphi_2 - \varphi_1}} (x - \varphi_1)^{\frac{1}{2}} & \varphi_1 \le x < \varphi_2 \\ K_\infty & \varphi_2 \le x \end{cases} \tag{17}$$

where, $0 \le x < \varphi_1$ represents the sticking state, $\varphi_1 \le x < \varphi_2$ represents the microslip state and $\varphi_2 \le x$ represents the macroslip state. The force-displacement relationship and stiffness-displacement relationship of the bolted joint with spigot are shown in the Fig. 4.

According to the above results, the slip process at the spigot can be divided into three stages: sticking, microslip and macroslip. There will stiffness loss at the microslip state with significant nonlinear characteristic. It's also known that the bolted joint with spigot contains three structural parameters, including **the microslip displacement** φ_1, **the macroslip displacement** φ_2 and **the stiffness loss coefficient** $\eta = K_\infty / K_0$, which all have decisive impacts on the mechanical characteristic of the bolted joint with spigot.

3 Dynamic Characteristic of the Non-continuous Rotor System

In this section, the dynamic response of a rotor system with a bolted joint with spigot has been calculated, which has been used to analyze the dynamic characteristic of the non-continuous rotor system.

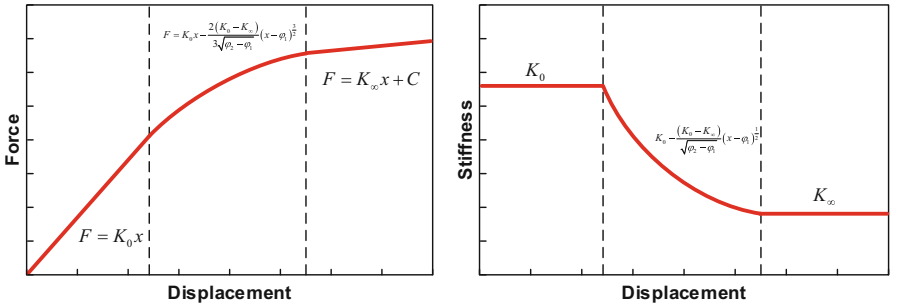

(a) Force-Displacement curve (b) Stiffness-Displacement curve

Fig. 4. Theoretical Derivation Results

3.1 The Rotor Example

A high-speed rotor system with two supporting has been selected as an example in this paper, as shown in the Fig. 5. There is a bolted joint with spigot at the drum shaft between the compressor and the turbine disk, which is the weakest structure of the rotor system. Therefore, the stiffness of the whole rotor system will be strongly influenced by the slip damage of this spigot interface.

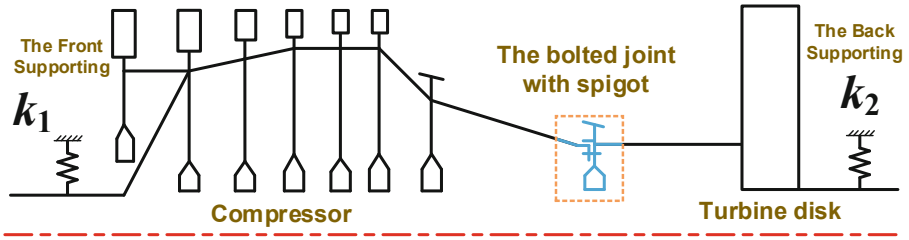

Fig. 5. Schematic diagram of The Rotor Example

The beam element model of the rotor system has been established, and the mass, stiffness, damping and gyroscope matrix have been respectively extracted. Based on the previous analysis, the force-displacement relationship during slippage has been substituted into the stiffness matrix, and a non-continuous rotor system with a bolted joint with spigot can be obtained.

The modal characteristic and unbalanced response of the continuous rotor system (the rotor example without considering the bolted joint with spigot) have been calculated, as shown in the Fig. 6.

According to the database, the rotor example operates at the range of about 11000~14000 rpm. As can be seen from the Fig. 6, the first and the second critical rotation speed are respectively 2790 rpm and 6630 rpm from the calculation results. Therefore, the operating rotation speed of the rotor system has been set between the second and the third critical rotation speed, and there will be low level dynamic response during the operating, which well satisfies the vibration requirement.

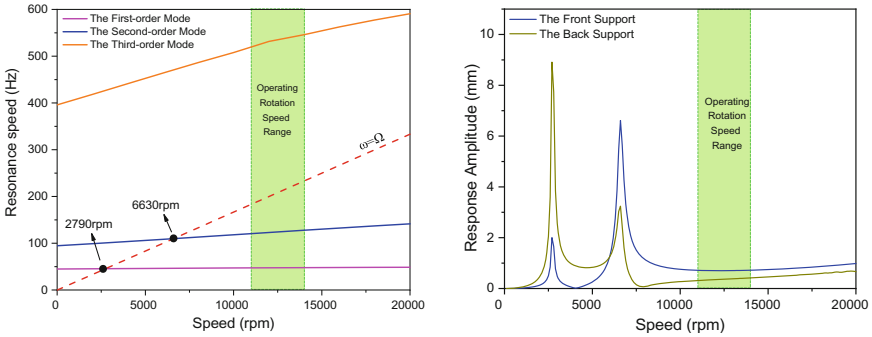

(a) The Modal Characteristic (b) The Unbalanced Response

Fig. 6. The Dynamic Characteristic of the Continuous Rotor System

3.2 The Slip Damage

Next, the bolted joint with spigot has been considered in the rotor example system, and the dynamic response has been calculated in the full rotation speed range.

It is known from the literature [20] that the magnitude of displacement of slip damage is within 10 μm. Therefore, the structural parameters have been taken separately the microslip displacement $\varphi_1 = 4\,\mu\text{m}$, the macroslip displacement $\varphi_2 = 6\,\mu\text{m}$ and the stiffness loss coefficient $\eta = 90\%$ in this calculation. The calculated non-continuous rotor dynamic response under the 100 g · mm unbalance has been calculated through the Newmark-β method, as shown in the Fig. 7.

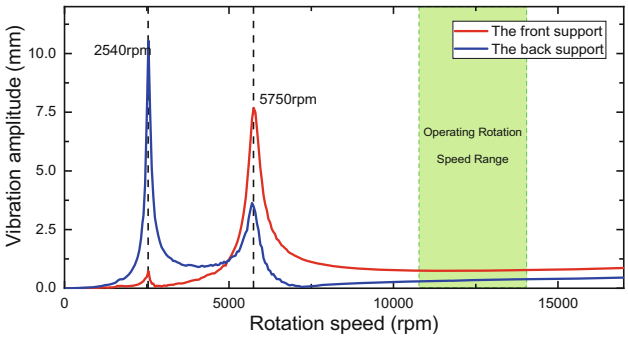

Fig. 7. The Dynamic Characteristic of the Non-Continuous Rotor System

Different from the calculation results of continuous rotor system, it can be found that the first and the second critical rotation speeds have descended respectively by 8.96% and 13.3% due to the slip damage of the bolted joint with spigot. In addition, the dynamic response at almost each speed has increased compared with the continuous rotor system.

It's necessary to pay attention to the change of the rotor whirl within the operating rotation speed range due to the slip damage of the bolted joint with spigot. It can be seen from the Fig. 8 that the bifurcation phenomenon of the dynamic response is relatively

obvious in the follow two situations: (1) in the low speed range and close to the first and the second critical rotation speed; (2) in the operating rotation speed range. For the former, which is caused by the large dynamic response; and for the latter, the cause is that the nonlinear characteristic of stiffness plays a leading role at the deformation range of the bolted joint.

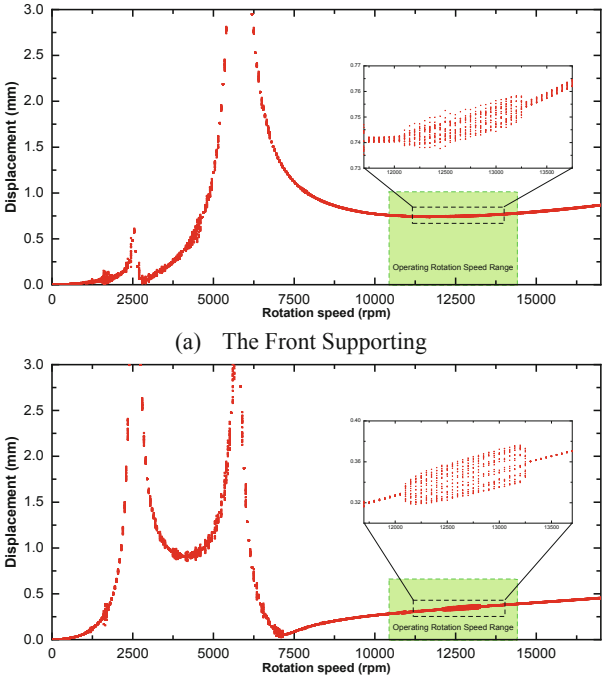

(a) The Front Supporting

(b) The Back Supporting

Fig. 8. Bifurcation diagram of the Non-Continuous Rotor System

The time, frequency and orbit responses at different rotation speeds have been extracted, as shown in the Fig. 9. It can be seen from the subgraph (a) that the response is large but the slip damage at the bolted joint with spigot is slight at the speed of 2500 rpm, which is close to the first critical rotation speed. The fundamental frequency dominated the frequency spectrum with the weak nonlinear characteristic of the rotor system.

As shown in the subgraph (b), the response has been significantly reduced as the rotation speed exceeds the second critical rotation speed. However, there has been the slip damage at the spigot interface because of the large deformation of the bolted joint with spigot, which made the non-circle orbit response. In addition, there are fundamental frequency and octave frequencies of rotational speed in the spectrum, which shows apparent nonlinear characteristic.

The nonlinear characteristic has become obvious due to the serious slip damage at the bolted joint with spigot in the operating rotation speed range as shown in the subgraph

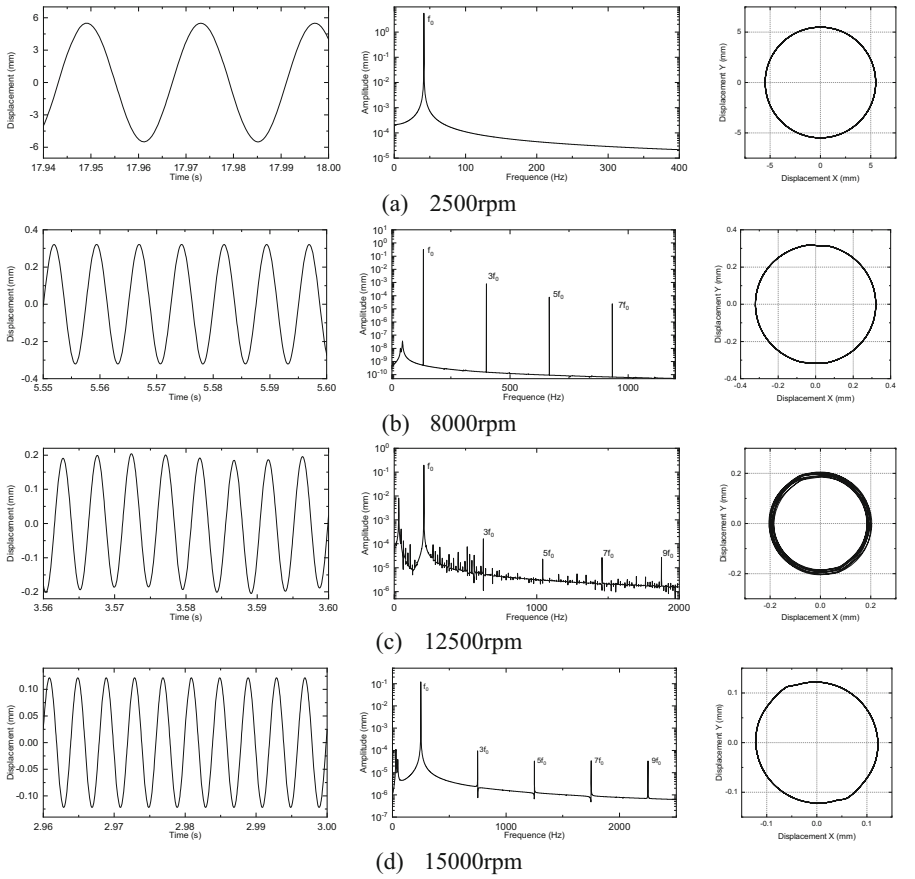

Fig. 9. Time, Frequency and Orbit Responses for different rotation speed

(c). The orbit response has become a ring with chaotic and irregular frequencies in the frequency response, which indicates the complex and unhealthy rotor whirl.

The slip damage at the bolted joint with spigot has depressed when the rotation speed is up to around 15000 rpm, as shown in the subgraph (d). Also, the nonlinear characteristic has weakened, which is similar to the response at the 8000 rpm shown in the subgraph (b).

Based on the previous analysis, it can be found that the impact of slip damage at the bolted joint with spigot is mainly concentrated in the specified rotation speed, rather than the whole rotation speed range. It's necessary to pay attention to the slip damage at the bolted joint with spigot while its effect concentrated on the operating rotation speed range.

3.3 Discussion

It can be known that structural parameters, such as microslip displacement φ_1, the macroslip displacement φ_2 and the stiffness loss coefficient η, have significant influence

on the rotor dynamic characteristic from the previous theoretical analysis. In addition, the value of excitation also has impact on the dynamic response on the non-continuous rotor system with the slip damage.

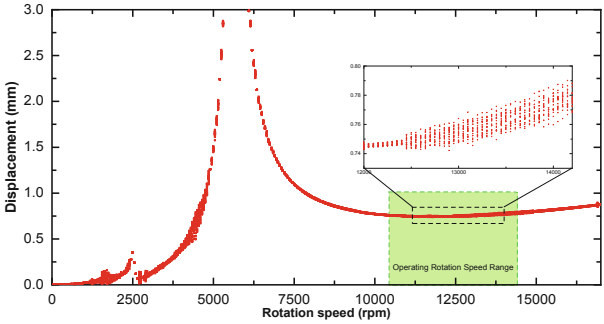

(a) The Front Supporting

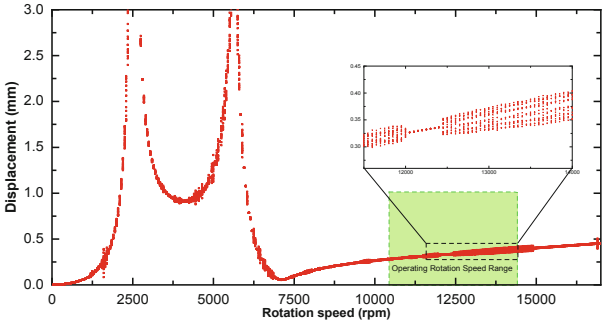

(b) The Back Supporting

Fig. 10. Bifurcation diagram of the Non-Continuous Rotor System with the different structural parameters

The structural parameters have been changed (microslip displacement $\varphi_1 = 6$ μm, the macroslip displacement $\varphi_2 = 8$ μm and the stiffness loss coefficient $\eta = 90\%$), and the dynamic response has shown in the Fig. 10. It can be known that the dynamic response at the most rotation speeds is similar to the previous results and the difference is concentrated at the operating rotation speed range, by compared with the Fig. 8 and Fig. 10. The most obvious is there is serious bifurcation phenomenon in the range of 12000 to 15000 rpm shown in the subgraph (b), which is little in the Fig. 8. Because of the similar response under different structural parameters, this paper will not repeat.

Similarly, the dynamic response can be changed by different value of excitation. It can be found from the Fig. 11 that the response amplitude is almost half of that shown in the Fig. 8 after the unbalance changed to 50 g·mm. However, the bifurcation phenomenon has changed during the operation rotation speed, which has strong performance at the back supporting. It can be seen from the subgraph (b) that there is slight bifurcation phenomenon at about 13000 rpm, but which has sharply strong after 13500 rpm and until 17000 rpm.

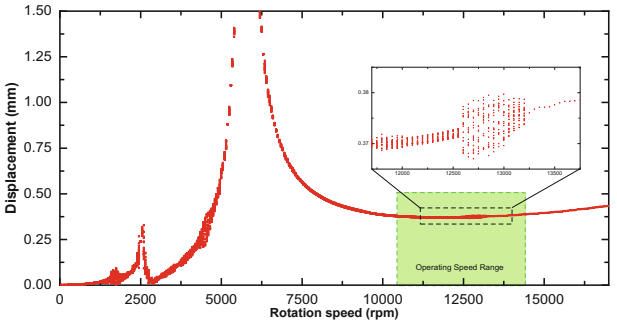

(a) The Front Supporting

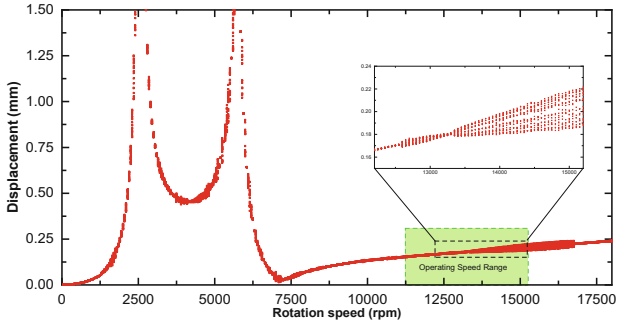

(b) The Back Supporting

Fig. 11. Bifurcation diagram of the Non-Continuous Rotor System under the 50 g·mm Unbalance

It can be found that when the structure parameters of the bolted joint with spigot and the value of excitation have changed, the rotation speed range and severity of bifurcation phenomenon will be greatly different through the above comparison. If thinking from another perspective, the adaptability of the rotor system to the slip damage can be adjusted by the robust design of the structure parameters of the bolted joint with spigot. Therefore, the author expresses a view that for the high-speed non-continuous rotor system, the slip damage is necessary to be considered in the design phase, and be placed in the appropriate rotation speed range through robust design, so as to ensure the robustness of the dynamic characteristic of the rotor system within the working speed range.

4 Conclusion

The bolted joint with spigot, as a widely used joint in aero-engine rotor system, has been lack of sufficient research of dynamic characteristic. The mechanical model has been proposed to analyze the slip damage during operating and the dynamic response of the non-continuous rotor system considering slip damage has been calculated in this paper. The results of this research have led to the following conclusions:

1) Aiming at the bolted joint with spigot, the slip damage mechanical model has been proposed to describe the process of the interface slippage and get the force-displacement relationship based on the Iwan model;

2) Based on the proposed mechanical model, the dynamic characteristic of the aero-engine rotor system considering the slip damage has been calculated. It has been found the prominent nonlinear characteristic during the slip damage, which is manifested as obvious bifurcation phenomenon.
3) The simulation of the non-continuous rotor system has indicated that the influence of the slip damage will vary according to the structure parameters and the value of excitation. It's necessary to fully consider the effect of slip damage in the rotor design stage to improve the robustness of rotor dynamic characteristic.

In this paper, a mechanical model of slip damage at bolted joint with spigot in the aero-engine rotor system has been established. However, due to the complexity of the load and structure of aero-engine, the depth analysis of the dynamic characteristic has been lack in this paper. In addition, the quantitative evaluation method of the influence of slip damage on the dynamic characteristic of aero-engine rotor system is also the future research direction.

References

1. Hong, J., Chen, X., Wang, Y., et al.: Optimization of dynamics of non-continuous rotor based on model of rotor stiffness. Mech. Syst. Signal Process. **131**, 166–182 (2019)
2. Hong, J., Ma, Y.: Structure and Design of Aircraft Gas Turbine Engine. Science Press, Beijing (2021)
3. Farrar, C.R., Worden, K.: An introduction to structural health monitoring. Philos. Trans. R. Soc. Lond. A: Math. Phys. Eng. Sci. **2007**(365), 303–315 (1851)
4. Brake, M.R.W. (ed.): The Mechanics of Jointed Structures. Springer, Cham (2018). https://doi.org/10.1007/978-3-319-56818-8
5. Gaul, L., Lenz, J.: Nonlinear dynamics of structures assembled by bolted joints. Acta Mech. **125**(1–4), 169–181 (1997)
6. Marshall, M.B., Lewis, R., Dwyerjoyce, R.S., et al.: Characterisation of contact pressure distribution in bolted joints (2006)
7. Iwan, W.D.: A Distributed-Element Model for Hysteresis and Its Steady-State Dynamic Response (1966)
8. Iwan, W.D.: On a Class of Models for the Yielding Behavior of Continuous and Composite Systems (1967)
9. Argatov, I.I., Butcher, E.A.: On the Iwan models for lap-type bolted joints. Int. J. Non Linear Mech. **46**(2), 347–356 (2011)
10. Kim, J., Yoon, J.C., Kang, B.S.: Finite element analysis and modeling of structure with bolted joints. Appl. Math. Model. **31**(8), 895–911 (2007)
11. Beaudoin, M.A., Behdinan, K.: Analytical lump model for the nonlinear dynamic response of bolted flanges in aero-engine casings. Mech. Syst. Signal Process. **115**, 14–28 (2019)
12. Ning, F.: Studies on Dynamic Characteristics of the Joint in the Aero-Engine Rotor System. BUAA, Beijing (2018)
13. Yue, W., Mei, Q., Zhang, D., et al.: Robust design method of rabbet joint structure in high speed assemble rotor. J. Aero-Space Power **32**(7), 1754–1761 (2017)
14. Cun, W.: Dynamic Model and Interval Analysis Method of Noncontinuous Rotor. BUAA, Beijing (2018)
15. Caddemi, S., Caliò, I.: Exact closed-form solution for the vibration modes of the Euler-Bernoulli beam with multiple open cracks. J. Sound Vib. **327**, 473–489 (2009)

16. Caddemi, S., Caliò, I., Cannizzaro, F.: Closed-form solutions for stepped Timoshenko beams with internal singularities and along-axis external supports. Arch. Appl. Mech. **83**, 559–577 (2013)
17. Hong, J., Yang, Z., Wang, Y., et al.: Combination resonances of rotor systems with asymmetric residual preloads in bolted joints. Mech. Syst. Signal Process. **183**, 109626 (2023)
18. Hong, J., Dai, Q., Wu, F., et al.: Dynamic characteristics analysis of flexible rotor system with pedestal looseness. In: Turbo Expo: Power for Land, Sea, and Air, vol. 85031, p. V09BT28A008. American Society of Mechanical Engineers (2021)
19. Lei, B., Li, C., Hong, J., Ma, Y.: Robust design of mechanical characteristics of rotor connection structure. Aeroengine **47**(02), 3844 (2021)
20. Hong, J., Ma, Y., Feng, S., et al.: The mechanism and quantitative evaluation of slip damage of bolted joint with spigot. In: ASME, Turbo Expo: Power for Land, Sea, and Air. American Society of Mechanical Engineers (2022)
21. Yu, P., Li, L., Chen, G., et al.: Dynamic modelling and vibration characteristics analysis for the bolted joint with spigot in the rotor system. Appl. Math. Model. **94**, 306–331 (2021)
22. Segalman, D.: A four parameter Iwan model for lap-type joints, Sandia report, SAND2002-3828. Sandia Laboratories, Albuquerque, NM (2002)
23. Segalman, D.J., Gregory, D.L., Starr, M.J., et al.: Handbook on dynamics of jointed structures. Sandia National Laboratories, Albuquerque (2009)